



# Mineral inclusions in rutile: A novel recorder of HP-UHP metamorphism

Emma Hart <sup>a,\*</sup>, Craig Storey <sup>a</sup>, Emilie Bruand <sup>a</sup>, Hans-Peter Schertl <sup>b</sup>, Bruce D. Alexander <sup>c</sup>

<sup>a</sup> School of Earth and Environmental Sciences, University of Portsmouth, Portsmouth, UK

<sup>b</sup> Ruhr-University Bochum, 44780 Bochum, Germany

<sup>c</sup> School of Science, University of Greenwich, Chatham Maritime, UK



## ARTICLE INFO

### Article history:

Received 7 December 2015

Received in revised form 16 April 2016

Accepted 21 April 2016

Available online 12 May 2016

Editor: M. Bickle

### Keywords:

rutile

mineral inclusions

(U)HP-LT metamorphism

subduction

coesite

## ABSTRACT

The ability to accurately constrain the secular record of high- and ultra-high pressure metamorphism on Earth is potentially hampered as these rocks are metastable and prone to retrogression, particularly during exhumation. Rutile is among the most widespread and best preserved minerals in high- and ultrahigh pressure rocks and a hitherto untested approach is to use mineral inclusions within rutile to record such conditions. In this study, rutiles from three different high- and ultrahigh-pressure massifs have been investigated for inclusions. Rutile is shown to contain inclusions of high-pressure minerals such as omphacite, garnet and high silica phengite, as well as diagnostic ultrahigh-pressure minerals, including the first reported occurrence of exceptionally preserved monomineralic coesite in rutile from the Dora-Maira massif. Chemical comparison of inclusion and matrix phases show that inclusions generally represent peak metamorphic assemblages; although rare prograde phases such as titanite, omphacite and corundum have also been identified implying that rutile grows continuously during prograde burial and traps mineralogic evidence of this evolution. Pressure estimates obtained from mineral inclusions, when used in conjunction with Zr-in-rutile thermometry, can provide additional constraints on the metamorphic conditions of the host rock. This study demonstrates that rutile is an excellent repository for high- and ultra-high pressure minerals and that the study of mineral inclusions in rutile may profoundly change the way we investigate and recover evidence of such events in both detrital populations and partially retrogressed samples.

© 2016 The Authors. Published by Elsevier B.V. This is an open access article under the CC BY license (<http://creativecommons.org/licenses/by/4.0/>).

## 1. Introduction

One of the most important and unresolved questions in the evolution of the Earth is the question of when did subduction-driven plate tectonics begin (e.g. Smart et al., 2016)? The magmatic record implies that subduction-driven plate tectonics began in the Archean *ca.* 3 Ga (e.g. Dhuime et al., 2012), while the metamorphic record, or more precisely the lack of (U)HP-LT rocks in the pre-Neoproterozoic, would suggest that the onset of modern subduction occurred after *ca.* 800 Ma (see Fig. 4 in Stern et al., 2013). (U)HP-LT rocks such as blueschists and UHP eclogites are the best direct lines of evidence geoscientists have for modern ‘cold and steep’ subduction, as opposed to the ‘hot and flat’ style of subduction proposed for the Archean (Stern, 2005). The oldest blueschists have been dated at about 800 Ma (Maruyama et al., 1996). However, there is a potential bias in the preservation of these rocks

with their absence in older crust possibly reflecting erosion or retrograde metamorphism (Stern et al., 2013). Recent studies have attempted to explain the lack of blueschists and UHP eclogites in the Paleoproterozoic and Archean, with modelling of different bulk rock chemistries of subducted crust suggesting that HP-LT rocks could have been present at that time (Palin and White, 2016).

To offer a way forward with the debate about when plate tectonics began, and to look beyond the Neoproterozoic for evidence of (U)HP-LT events, we have developed a new way of utilising rutile. Rutile is a robust accessory mineral that is stable over a large *P-T* range and is commonly found in HP-UHP blueschists and eclogites (Meinhold, 2010). Unlike zircon, information derived from rutile reflects the conditions of the last metamorphic event, as during new metamorphic cycles rutile reacts to form other Ti-rich phases under greenschist-facies conditions (e.g. Zack et al., 2004; Triebold et al., 2007). Its resistance to retrogression can give an insight into the metamorphic history of a rock, particularly where evidence of metamorphism has been partially obliterated in the matrix. The robust nature of rutile during diagenetic processes also makes it a useful tool in sedimentary provenance studies as it re-

\* Corresponding author.

E-mail address: [emma.hart@port.ac.uk](mailto:emma.hart@port.ac.uk) (E. Hart).

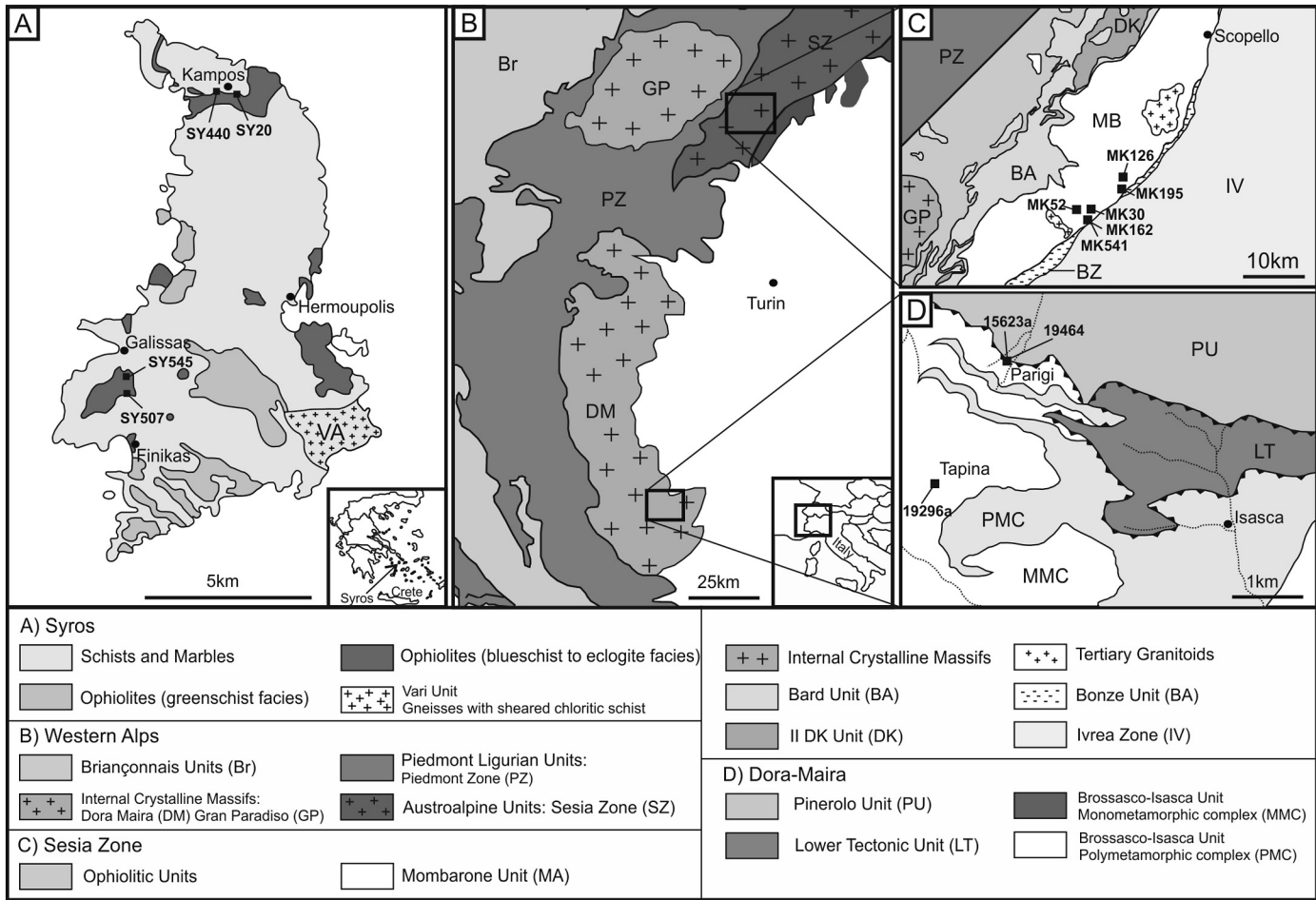


**Fig. 1.** Simplified geological maps of the three areas chosen for this study: (a) Syros (modified after Marschall et al., 2006); (b) Regional map of the Western Alps (after Schmid et al., 2004; Gasco et al., 2013), the location of the Sesia Zone and Dora-Maira study areas are indicated by the open boxes; (c) Sesia Zone (after Konrad-Schmolke et al., 2006); (d) Dora-Maira massif (after Compagnoni et al., 1994; Schertl and Schreyer, 2008).

tains geochemical information from the source rock. It has a strong affinity for high field strength elements, such as Nb, Ta and Cr, which can be useful in determining source rock lithology (Zack et al., 2004; Triebold et al., 2007). It can also be dated using the U-Pb system (e.g. Zack et al., 2011), and metamorphic temperatures of rutile growth can be obtained using the Zr-in-rutile geothermometer with an appropriate calibration (e.g. Tomkins et al., 2007).

In this contribution, mineral inclusions preserved in rutile from three localities have been systematically characterised to look for evidence of HP-UHP metamorphism (Syros, Greece; Sesia Zone and Dora-Maira massif, Western Alps). Although rutile has a distinct [110] cleavage and a tendency for twinning, two aspects which are potentially harmful for inclusions, it is shown here that rutile is a surprisingly good shelter for phases which are easily destroyed during exhumation, and establishes rutile as another phase (besides garnet and zircon) which is able to preserve evidence of UHP metamorphism via mineral inclusions. This study also demonstrates that mineral inclusions can provide additional *P-T* information when used in conjunction with existing methods, and discusses the potential of using detrital rutile to find evidence of HP-UHP events in eroded source terranes.

## 2. Geological settings

### 2.1. Syros, Greece

The Island of Syros (Fig. 1a) forms part of the lower unit of the Attic-Cycladic Crystalline Complex within the Hellenic orogeny

(Tomaschek et al., 2003), which preserves high-pressure metamorphic assemblages (e.g. Marschall et al., 2006). Subduction during the Eurasia–Africa collision at 50–54 Ma (Tomaschek et al., 2003) resulted in blueschist- to eclogite-facies high-pressure metamorphism, with peak conditions reaching 450–540 °C at 15–20 kbar (Okrusch and Bröcker, 1990; Trotet et al., 2001). Syros comprises several tectonostratigraphic units which include pre-Alpidic basement, marbles and schists, volcanosedimentary sequences, along with slices of blueschist- to eclogite-facies ophiolites which are exposed around the Island (Fig. 1a; Tomaschek et al., 2003). These slices of ophiolites are made up of serpentinites, metagabbros, metagranites and metasediments (Marschall et al., 2006). The four samples used in this study come from two different ophiolites; two metasomatized metabasites were taken from the north of the Island near Kampus, with an eclogite- and a blueschist-facies metabasite taken from south of Galissas (Fig. 1a).

### 2.2. Sesia Zone, Western Alps

The Sesia Zone forms part of the Austro-Alpine units and represents the largest slice of subducted continental crust during the Alpine orogeny (Rubatto et al., 1999; Konrad-Schmolke et al., 2006; Fig. 1b). It predominantly comprises a polymetamorphic metasedimentary basement which has been intruded by granitoids and Pre-Alpine mafic bodies (Rubatto et al., 1999). The Sesia Zone has been subdivided into four lithotectonic units: The Mombarone Unit, Bard Unit, Bonze Unit and the II DK Unit (Konrad-Schmolke et al., 2006; Fig. 1c). For this study, samples were obtained from the Mom-

barone unit, also described as the Eclogitic Micaschist Complex by Compagnoni et al. (1977). A widely accepted age for the peak metamorphism is ~65 Ma (Rubatto et al., 1999) with metamorphic conditions in the Mombarone unit reaching ~500–600 °C and 11–23 kbar (Compagnoni et al., 1977; Pognante, 1989; Rubatto et al., 1999; Tropper et al., 1999; Konrad-Schmolke et al., 2006). Six micaschists were collected in the southern part of the unit, along the boundary between the Mombarone Unit and the Ivrea Zone (Fig. 1c).

### 2.3. Dora-Maira massif, Western Alps

The Dora-Maira massif is one of three Internal Crystalline Massifs within the Penninic domain of the Western Alps (Gebauer et al., 1997; Fig. 1b), comprising Pre-Alpine basement rocks and Mesozoic cover (Chopin, 1984; Schertl and Schreyer, 2008). Metamorphic coesite was first described in the Dora-Maira massif (Chopin, 1984), which is known worldwide as its type locality. The coesite-bearing rocks are found in the Brossasco-Isasca Unit (BIU; Compagnoni et al., 1994) of the southern part of the Massif. The unit has been subdivided into a polymetamorphic and a monometamorphic complex by Compagnoni et al. (1994). The samples studied here (coesite-bearing pyrope quartzite and two pyrope megablasts) are restricted to the monometamorphic complex, which underwent UHP metamorphism at ~35 Ma (e.g., Duchêne et al., 1997; Gebauer et al., 1997). The pyrope-bearing rocks were collected at two localities (Fig. 1d): the classical type locality for metamorphic coesite at Parigi/Case Ramello (Chopin, 1984; Compagnoni et al., 1994) and at Tapina, ca 2 km SW of Parigi (Simon et al., 1997; Schertl and Schreyer, 2008). Peak metamorphic conditions of 720–800 °C and 36–37 kbar have been proposed, based upon the preservation of UHP minerals (Chopin et al., 1991; Schertl et al., 1991; Compagnoni et al., 1994; Nowlan et al., 2000).

## 3. Analytical techniques

Rutiles were prepared for analysis in two ways: 1) as mineral separates using standard rock crushing and heavy mineral separation techniques, which were picked, mounted and polished within epoxy resin-mounted grains, and 2) within polished thick sections (ca. 100 µm). Rutile separates were used to make the task of finding true inclusions easier and statistically more robust. Information regarding the number of analysed rutile separates and the percentages of those with inclusions can be found in Table 1. All images were collected using a JEOL JSM-6100 scanning electron microscope (SEM) with qualitative mineral chemical analyses performed using an Oxford Instruments energy dispersive spectrometer (EDS) at the University of Portsmouth. Inclusions in rutile separates were then quantitatively analysed for mineral chemistry, and matrix analyses obtained from thin sections, using a Cameca SX100 electron microprobe at the University of Bristol. Some inclusions were further analysed using a Horiba Jobin Yvon Raman microscope fitted with frequency-doubled Nd:YAG (532 nm) and HeNe (633 nm) lasers at the University of Greenwich. Laser ablation inductively coupled plasma mass spectrometry (LA-ICP-MS) was carried out at the University of Portsmouth using an Agilent 7500cs (quadrupole) ICP-MS coupled with a New-Wave UP213 ( $\lambda = 213$  nm) solid state Nd:YAG laser. For a more detailed description of the techniques used see supplementary material (Appendix A).

## 4. Sample descriptions

### 4.1. Syros, Greece

Sample SY440 is a metasomatized metabasalt comprising omphacite, chlorite, rutile and apatite and sample SY507 is an

**Table 1**  
Sample localities, matrix mineral assemblages, inclusion assemblages and  $P-T$  estimates taken from the literature. Abbreviations after Whitney and Evans (2010): albite (Ab), apatite (Ap), chlorite (Chl), coesite (Coe), corundum (Crn), ellénbergerite (Eb), epidote (Ep), garnet (Gt), glaucophane (Gln), hematite (Hem), ilmenite (Ilm), kyanite (Ky), monazite (Mnz), omphacite (Omp), paragonite (Pg), quartz (Qtz), rutile (Rt), talc (Tlc), titanite (Ttn), zircon (Zrn).

Locality	Rock type	Mineral assemblage	Accessory	$P-T$ estimates		% Inclusion	% Without	Primary	Secondary	
				T	P				Ilm	Chl
Syros, Greece										
SY440	Mafic	Omp-Chl-Ep	Rt-Ap	400–550	5–20	20	45	55	Qtz-Gt-Gln	Qtz-Gt-Ab-Phe-Pg-Gln-Zrn
SY507	Mafic	Gt-Omp-Phe-Ep-Chl	Rt-Ttn-Ap-Zrn			70	37	63		
SY545	Mafic	Gt-Gln-Phe-Qtz-Ep				70	99	1		
Sesia Lanzo, Western Alps										
MK30	Pelitic	Gln-Gt-Qtz-Phe-Ep	Rt-Ap-Zrn	500–600	11–23	63	21	79	Qtz-Gt-Gln	Qtz-Gt-Ab-Phe-Pg-Gln-Zrn
MK52	Pelitic	Gln-Gt-Qtz-Phe-Ab-Ep	Rt-Ttn-Ap			50	50	50		
MK126	Pelitic	Gt-Phe-Qtz-Gln-Ab-Chl-Omp	Rt-Ttn-Zrn			59	49	51		
MK162	Pelitic	Gt-Phe-Qtz-Gln-Pg-Ep-Chl	Rt-Ttn-Zrn			50	34	66		
MK195	Pelitic	Gt-Phe-Qtz-Gln	Rt-Ttn-Zrn			79	42	58		
MK541	Pelitic	Omp-Gt-Qtz-Phe-Gln-Ab-Ep	Rt-Ttn-Zrn			59	29	71		
Dora-Maira, Western Alps										
15623a	Metasomatic	Gt-Ky-Tlc-Chl-Eb	Rt-Zrn	720–800	36–37	21	29	71	Gt	Qtz-Gt-Phe-Ky-Zrn
19296a	Metasomatic	Gt-Qtz/Coe-Ky-Phe-Tlc	Rt-Zrn-Mnz			52	13	87		
19464	Metasomatic	Gt-Qtz/Coe-Ky-Phe-Tlc	Rt-Zrn-Mnz			72	11	89		

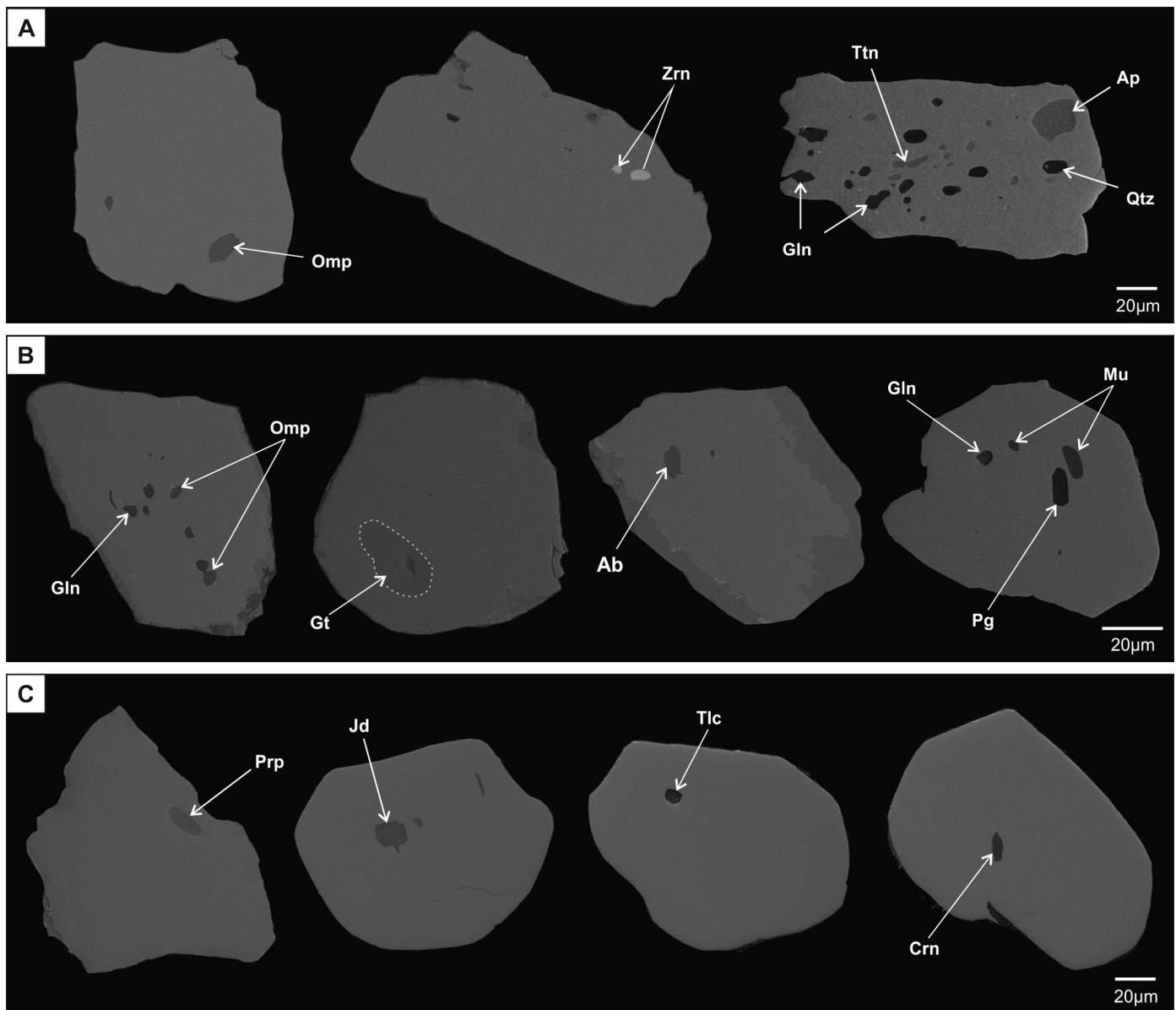


**Fig. 2.** BSE images of rutiles with inclusions from (a) Syros; (b) Sesia Zone and (c) Dora–Maira. For a full list of abbreviations see Table 1.

eclogite-facies metagabbro comprising garnet, omphacite and rutile with minor amounts of epidote, chlorite and titanite which are a product of fluid–rock interaction and retrogression. Sample SY545 on the other hand, is a blueschist-facies meta-igneous glaucophane schist, comprising garnet, glaucophane, quartz, and phengite as part of the peak paragenesis, along with rutile, zircon and apatite as accessory minerals (Table 1). Titanite and epidote occur as retrograde phases. Rutiles in the Syros samples occur as small (1–4 mm) idioblastic grains (Fig. 2a). The smaller grains are found both as inclusions in garnet and in the matrix; whereas, the large grains occur only in the matrix.

#### 4.2. Sesia Zone, Western Alps

The six samples from the Mombarone Unit in the Sesia Zone are metapelitic garnet–glaucophane micaschists that have undergone blueschist- to eclogite-facies metamorphism. All of the samples are fine- to medium-grained and their peak assemblages include garnet, quartz, phengite and glaucophane. Samples MK52, MK126 and

MK541 additionally contain albite and samples MK126 and MK541 contain omphacite. Paragonite is also found within the matrix of sample MK162. Accessory minerals include rutile, titanite, zircon and apatite (Table 1). Epidote and chlorite may be present and are products of greenschist-facies retrogression. Rutile grains in the Sesia Zone samples are generally elongated and well rounded, ranging from 40–600 µm in length (Fig. 2b), and show a preferred orientation parallel to the strong lineation defined by white mica and quartz. Rutile occurs within the matrix of the samples only, except in samples MK52 and MK162 where it is also found as small inclusions within garnet. Most grains are partially replaced by late titanite at their rims.

#### 4.3. Dora–Maira massif, Western Alps

The two outcrops studied are made up of both fine-grained and coarse-grained metasomatic pyrope-bearing quartzites, with pyrope megablasts in the coarse-grained quartzite reaching up to 25 cm in diameter (Chopin, 1984; Schertl et al., 1991). The pyrope megablasts were formed in a silica deficient environment and

contain inclusions of kyanite, chlorite and talc in addition to a variety of unusual minerals (e.g. ellenbergerite). For detailed descriptions see Schertl et al. (1991). The common mineral assemblage for the pyrope quartzite is garnet, kyanite, phengite, quartz/coesite, talc, jadeite, with rutile, zircon, and monazite as accessory phases (Chopin, 1984; Schertl et al., 1991; see Table 1). Phengite has a high concentration of Si (up to 3.57 a.p.f.u.), garnet is of nearly pure pyrope composition ( $\text{Alm}_{03} \text{Prp}_{97}$ ) and the jadeite component within clinopyroxene reaches 88 mol%. Rutile from samples 15623a (Parigi/Case Ramello) and 19296a (Tapina) were both separated from large pyrope megablasts. Sample 19464 (Parigi/Case Ramello) on the other hand is from a fine-grained pyrope quartzite. Rutile is found within the matrix as well as within garnet and occurs as 50–800  $\mu\text{m}$  in diameter idioblastic to well-rounded xenoblastic grains (Fig. 2c).

## 5. Mineral inclusions

An ideal primary inclusion is defined as being monomineralic, rounded and completely surrounded by the host (the host being crack-free). Although some inclusions are close to the rims of some rutile grains and could have been in contact with the matrix in 3D, many are not and we have been careful to check that we have not relied on interpretations from any inclusion suites that we are not confident are well within the grain boundary. Information regarding the number of rutile separates analysed per sample and percentages of rutile that contain inclusions is summarized in Table 1. In terms of abundance, 'common' is defined as more than 10 identified primary inclusions per sample and 'rare' as less than 10 inclusions.

Rutile separates from each of the twelve studied samples were analysed for mineral inclusions (Table 1). Of all the studied samples, SY545, a blueschist-facies metabasite from Syros, has the highest proportion of inclusion-bearing rutile, with 99% of analysed grains containing inclusions (Table 1). Rutiles from this sample also contain the most inclusions, typically with more than ten monomineralic inclusions of up to four different types per grain (Fig. 2a). In this sample, common primary inclusions comprise glaucophane, titanite and quartz, with rare inclusions of apatite and zircon (Fig. 2a; Table 1). Although titanite is often associated with retrogression in the matrix, the titanite inclusions observed in this sample are monomineralic, in a crack-free host and have no connection to the matrix and are therefore interpreted to be prograde (Fig. 2a). In comparison, the two other samples from Syros (SY440 and SY507) have a lower proportion of inclusion-bearing rutile. Omphacite is the most common inclusion constituting >80% of identified inclusions, with rare inclusions of zircon and secondary chlorite and ilmenite (Table 1).

Rutiles from the six Sesia Zone samples have up to 50% of analysed grains containing inclusions (Fig. 2b; Table 1). Common primary inclusions comprise glaucophane, phengite, albite and quartz. Rare inclusions of garnet, paragonite, omphacite, zircon and apatite are also present as well as secondary titanite and ilmenite (Table 1). Omphacite inclusions are found within samples MK162 and MK195 despite the absence of omphacite in the matrix.

Mineral inclusions within rutile from the Dora-Maira massif are rare and when present there is typically only one inclusion per grain (Fig. 2c). Rutile separates from pyrope megablasts contain a limited amount of inclusions with only rare inclusions of pyrope garnet identified in sample 15623a and rare inclusions of quartz, pyrope, phengite, kyanite and zircon in sample 19296a (Table 1). Rutile separated from the matrix of the fine-grained pyrope quartzite from Parigi/Case Ramello (sample 19464) contain a wider variety of inclusions with rare quartz/coesite, phengite, garnet, kyanite, jadeite, talc corundum and zircon (Table 1). Unlike the other inclusions, corundum is not present in the matrix. Co-

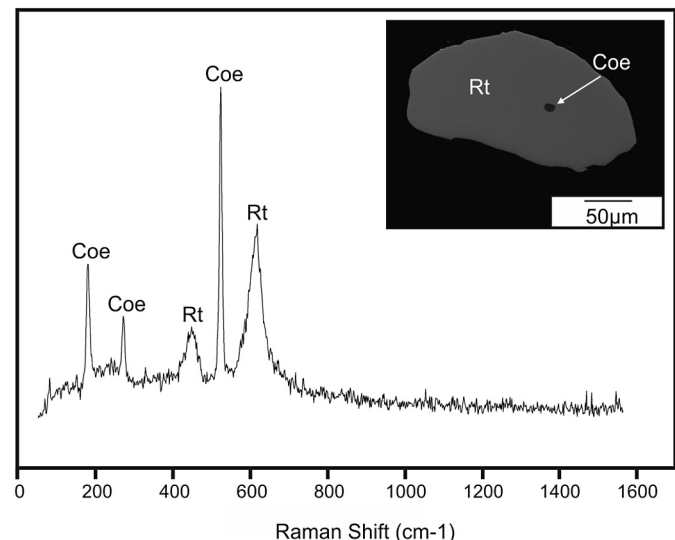


**Fig. 3.** Representative Raman spectra and a BSE image of a coesite inclusion within rutile from the Dora-Maira massif (sample 19464).

esite inclusions were identified in five rutile grains using Raman spectroscopy (Fig. 3). Coesite inclusions are typically 10  $\mu\text{m}$  in diameter and occur as ovoid inclusions (inset of Fig. 3). No radial fractures are observed around the inclusions, indicating preservation of coesite rather than partial phase transformation to the larger volume quartz polymorph. Coesite is easily distinguished by the large Raman shift which occurs around 523  $\text{cm}^{-1}$ , with two of the smaller peaks at 270  $\text{cm}^{-1}$  and 179  $\text{cm}^{-1}$  (Fig. 3). Two rutile bands at 447  $\text{cm}^{-1}$  and 616  $\text{cm}^{-1}$  are also present within the spectra due to interference caused by the reflectance of the host rutile.

### 5.1. Inclusion vs matrix chemistry

Representative electron microprobe analyses of key inclusion and matrix phases are presented in Table 2, which shows that primary inclusions found within rutile generally match those minerals found within the matrix of the respective samples. Phengite in the matrix of sample 19464 from the Dora-Maira massif for example, is characterised by high Si contents of up to 3.49 a.p.f.u. and high  $X_{\text{Mg}}$  ratios around 0.98 which are indicative of UHP conditions and diagnostic of the Mg-rich protolith. Equivalent high Si contents are also recorded in phengite inclusions (Table 2), which is similar to observations made in a previous study (Schertl and Schreyer, 1996). Phengite in the matrix of sample MK126 from the Sesia Zone has lower Si and  $X_{\text{Mg}}$  contents of 3.39 a.p.f.u. and 0.77, respectively. Similar values are also recorded in phengite inclusions from the rutile separates and again show that inclusion chemistry is comparable to the matrix.

Compositions of omphacite for samples SY440 and SY507 are plotted in a  $X_{\text{Mg}}$  vs  $X_{\text{Jd}}$  diagram (Fig. 4). Omphacites in the matrix of sample SY440 have  $X_{\text{Mg}}$  ratios of 0.45–0.53, whereas matrix omphacites in sample SY507 have slightly higher  $X_{\text{Mg}}$  ratios of 0.54–0.62. Inclusions in rutile from SY440 have  $X_{\text{Mg}}$  ratios of 0.47–0.50 and inclusions in SY507 have ratios of 0.53–0.64, therefore the  $X_{\text{Mg}}$  ratios recorded in omphacite inclusions match the matrix composition. Matrix and inclusion omphacites from sample SY440 have an average jadeite content ( $X_{\text{Jd}}$ ) of 0.34, whereas omphacites from SY507 have an average of 0.32.

The chemical compositions of garnet (inclusions vs matrix) are plotted on a ternary diagram (Fig. 5a). In samples MK30, MK162 and MK195, where matrix garnet is fairly homogeneous, inclusion and matrix analyses are comparable (Fig. 5a; Table 2). In sample

**Table 2**

Representative EPMA data of key phases found as inclusions (In) compared to matrix (Mx) analyses.

Omphacite				Glaucophane				Garnet				Paragonite		Phengite				Pyrope				Jadeite				
SY440		SY507		SY545		MK30		MK195		MK541		MK162		MK126		19464		15623a		19296a		19464				
In	Mx	In	Mx	In	Mx	In	Mx	In	Mx	In	Mx	In	Mx	In	Mx	In	Mx	In	Mx	In	Mx	In	Mx			
SiO <sub>2</sub>	55.1	55.8	54.7	54.6	57.1	57.9	57.0	58.6	37.0	37.4	36.8	37.1	37.3	46.5	46.8	49.1	51.2	52.2	51.8	44.3	45.0	43.6	44.4	57.4	57.7	
TiO <sub>2</sub>	0.6	0.1	1.0	0.1	0.8	0.0	1.3	0.0	0.8	0.0	0.4	0.6	0.1	0.8	0.1	0.5	0.4	1.5	0.4	0.1	0.0	0.1	0.0	0.7	0.7	
Al <sub>2</sub> O <sub>3</sub>	8.8	8.5	8.2	8.5	11.3	11.0	12.4	12.5	21.3	20.9	21.2	21.6	21.4	39.8	39.2	29.8	28.2	25.6	24.3	25.2	24.9	25.3	25.0	22.6	22.2	
FeO	11.2	10.9	10.1	9.1	8.9	9.4	7.9	7.4	31.4	31.0	33.3	28.4	31.5	0.2	0.4	1.8	1.7	0.2	0.2	3.6	1.4	1.8	3.2	0.5	0.4	
MnO	0.2	0.1	0.0	0.0	0.0	0.1	0.0	0.0	1.0	0.7	1.0	1.0	0.9	0.0	0.0	0.0	0.0	0.0	0.0	0.1	0.0	0.0	0.0	0.0	0.0	
MgO	5.6	5.8	7.0	7.3	11.2	11.3	11.0	10.8	2.5	1.9	2.7	1.9	3.4	0.1	0.1	2.6	3.2	5.7	6.3	28.4	29.3	29.7	27.7	3.8	3.6	
CaO	9.9	10.4	11.8	12.1	1.0	0.7	0.6	0.6	6.5	8.6	4.9	10.6	6.4	0.1	0.2	0.1	0.0	0.0	0.0	0.1	0.1	0.2	0.6	2.8	2.9	
Na <sub>2</sub> O	8.7	8.2	8.0	7.4	7.3	7.1	7.2	7.0	0.1	0.1	0.0	0.0	0.0	7.7	7.5	0.5	0.9	0.2	0.0	0.0	0.0	0.0	0.1	12.1	12.0	
K <sub>2</sub> O	0.0	0.0	0.0	0.0	0.0	0.0	0.0	0.0	0.0	0.0	0.0	0.0	0.0	0.3	0.6	9.8	9.8	10.5	10.6	0.0	0.0	0.0	0.0	0.0	0.0	
Σ	99.9	99.8	100.7	99.3	97.7	97.7	97.8	96.9	100.6	100.5	100.4	101.2	101.2	95.6	95.0	94.4	95.4	96.7	93.6	101.7	100.7	101.0	101.0	100.0	99.7	
O	6	6	6	6	23	23	23	23	12	12	12	12	12	11	11	11	11	11	11	12	12	12	12	6	6	
Si	2.0	2.0	2.0	2.0	7.8	7.9	7.8	8.0	2.9	3.0	2.9	2.9	2.9	3.0	3.0	3.3	3.39	3.4	3.49	3.0	3.0	2.9	3.0	2.0	2.0	
Ti	0.0	0.0	0.0	0.0	0.1	0.0	0.1	0.0	0.0	0.0	0.0	0.0	0.0	0.0	0.0	0.0	0.1	0.0	0.0	0.0	0.0	0.0	0.0	0.0	0.0	
Al	0.4	0.4	0.3	0.4	1.8	1.8	2.0	2.0	2.0	2.0	2.0	2.0	2.0	3.0	3.0	2.4	2.2	2.0	1.9	2.0	2.0	2.0	2.0	0.9	0.9	
Fe <sup>3+</sup>	0.2	0.2	0.3	0.2	0.0	0.0	0.0	0.0	0.0	0.1	0.1	0.1	0.1	0.0	0.0	0.0	0.0	0.0	0.0	0.0	0.0	0.0	0.0	0.0	0.0	
Fe <sup>2+</sup>	0.1	0.2	0.0	0.1	1.0	1.1	0.9	0.8	2.1	2.0	2.2	1.8	1.9	0.0	0.0	0.1	0.1	0.0	0.0	0.2	0.1	-0.1	0.2	0.0	0.0	
Mn	0.0	0.0	0.0	0.0	0.0	0.0	0.0	0.0	0.1	0.0	0.1	0.1	0.1	0.0	0.0	0.0	0.0	0.0	0.0	0.0	0.0	0.0	0.0	0.0	0.0	
Mg	0.3	0.3	0.4	0.4	2.3	2.3	2.2	2.2	0.3	0.2	0.3	0.2	0.4	0.0	0.0	0.3	0.3	0.6	0.6	2.8	2.9	3.0	2.8	0.2	0.2	
Ca	0.4	0.4	0.4	0.5	0.2	0.1	0.1	0.1	0.6	0.7	0.4	0.9	0.5	0.0	0.0	0.0	0.0	0.0	0.0	0.0	0.0	0.0	0.0	0.1	0.1	
Na	0.6	0.6	0.6	0.5	1.9	1.9	1.9	1.8	0.0	0.0	0.0	0.0	0.0	0.9	0.9	0.1	0.1	0.0	0.0	0.0	0.0	0.0	0.0	0.8	0.8	
K	0.0	0.0	0.0	0.0	0.0	0.0	0.0	0.0	0.0	0.0	0.0	0.0	0.0	0.0	0.0	0.8	0.8	0.9	0.9	0.0	0.0	0.0	0.0	0.0	0.0	
Σ	4.0	4.0	4.0	4.0	15.1	15.1	15.1	15.0	8.0	8.0	8.0	8.0	8.0	7.0	7.0	6.9	7.0	7.0	7.0	8.0	8.0	8.0	8.0	4.0	4.0	
Alm									70	67	74	61	67							7	3	3	6			
Prp									10	7	10	7	13							93	97	96	93			
Gr									19	24	14	29	18							0	0	0	2			
Sps									2	2	2	2	2							0	0	0	0			
Ag	24	18	25	21																	0	0				
Jd	38	41	30	32																	89	88				
Di	39	41	45	47																	11	12				

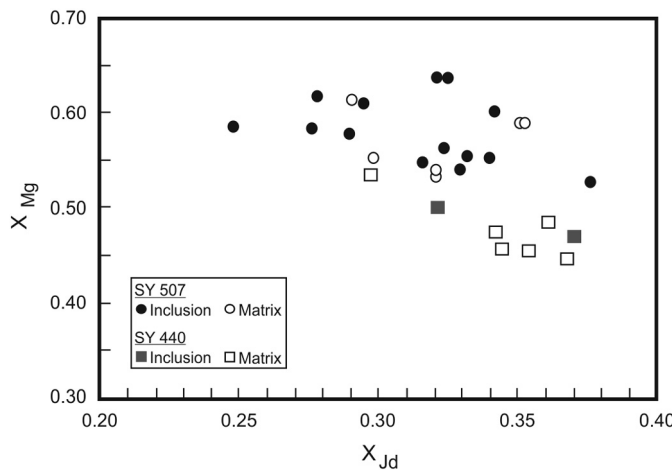


**Fig. 4.**  $X_{Mg}$  vs  $X_{Jd}$  diagram comparing the chemical composition of matrix and inclusion omphacite for samples from Syros (SY440 and SY507).

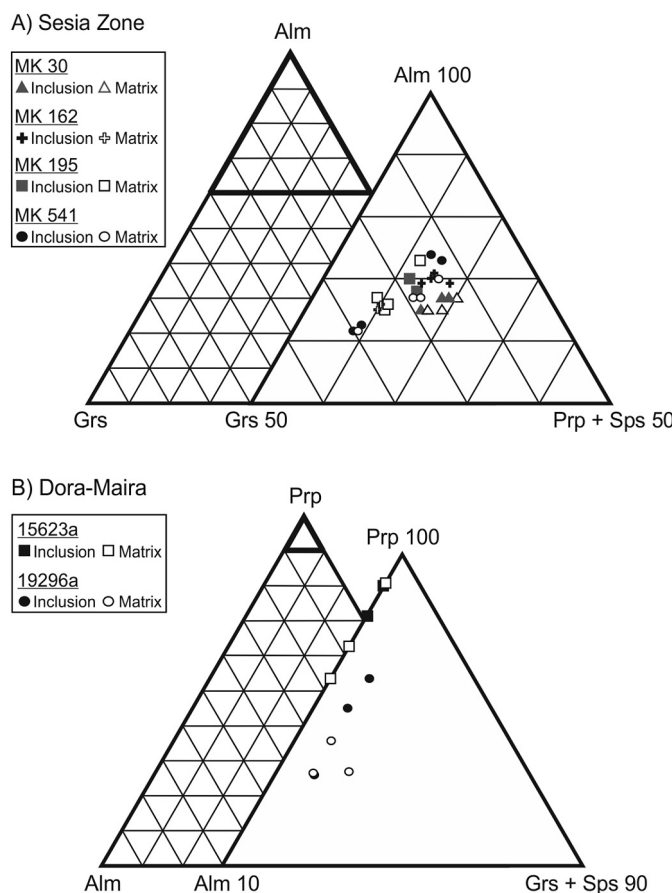


**Fig. 5.** Ternary diagrams showing the chemical composition of matrix and inclusion garnet: (a) Almandine – (Pyrope + Spessartine) – Grossular ternary diagram of garnets from the Sesia Zone; (b) Pyrope – (Grossular + Spessartine) – Almandine ternary diagram of garnets from the Dora-Maira massif.

MK541 however, two compositions of garnet are recorded in inclusions; both that of the matrix garnet ( $Alm_{74} Prp_{10} Grs_{14} Sps_{02}$ ) and one which contains more grossular and less almandine ( $Alm_{61} Prp_{07} Grs_{29} Sps_{02}$ ) (Fig. 5a; Table 2). Garnet compositions have also been obtained from some pyrope garnets from the Dora-Maira massif (Fig. 5b). Comparable analyses between inclusions and matrix are observed in sample 19296a where both have an average composition of  $Alm_5 Prp_{94} Grs_1$ . The average composition of ma-

trix pyrope in sample 15623a is  $Alm_4 Prp_{96}$ , while inclusions have a slightly higher pyrope end-member ( $Alm_1 Prp_{99}$ ; Fig. 5b).

## 6. Thermobarometry

The Zr-in-rutile thermometer is a reliable method for obtaining precise single grain temperature estimates of rutile growth. However, there is currently no way of determining pressures from rutile alone which is important as the thermometer has a small but not insignificant pressure dependency that requires correction (Tomkins et al., 2007). This study demonstrates that pressure estimates can be obtained from mineral inclusions and show how this additional information can be used in conjunction with Zr-in-rutile thermometry to obtain accurate  $P-T$  estimates for both detrital rutile and rutile from partially retrogressed samples. We also show that under certain circumstances, average  $P-T$  estimates using THERMOCALC can be applied to suites of mineral inclusions within rutile grains from individual samples.

### 6.1. Zr-in-rutile thermometry

The use of Zr-in-rutile thermometry in metamorphic rocks is particularly appealing as rutile occurs as an accessory mineral in many high-pressure metamorphic assemblages and is involved in metamorphic reactions which can be used as indicators of  $P-T$  conditions. The partitioning of Zr into rutile has proven to be strongly temperature dependent in rocks that contain the assemblage rutile-zircon-quartz (e.g. Tomkins et al., 2007). The chemical potential of  $ZrO_2$  is fixed, thus variations in Zr content can be attributed to changes in temperature. For accurate and precise results, ideal activity of Ti, Si and Zr must be demonstrated as it is an internally-buffered system (e.g. Tomkins et al., 2007). In this study, this condition is satisfied in some samples by the presence of co-existing quartz/coesite and zircon within the different samples (Table 1). For the purpose of this paper the calibration of Watson et al. (2006) has been used to demonstrate the applicability of Zr-in-rutile thermometry to detrital grains and retrogressed rocks. For trace element data and individual Zr-in-rutile temperatures please see supplementary materials (Table B.1).

Rutile from sample SY440 has Zr-concentrations ranging between 34–54 ppm, corresponding to temperatures of  $493\text{--}521 \pm 28^\circ\text{C}$ ; whereas, sample SY507 has 43–59 ppm Zr which gives temperatures of  $507\text{--}527 \pm 28^\circ\text{C}$ . The absence of quartz and zircon within the matrix of samples SY440 and SY507 means that the temperatures obtained should be treated as minimum estimates. Despite this, temperatures obtained are within the range of peak metamorphic temperature estimates from the literature ( $450\text{--}540^\circ\text{C}$ ; Okrusch and Bröcker, 1990; Trotet et al., 2001). Rutiles from the blueschist-facies sample SY545, which unlike the other samples from Syros grew in coexistence with quartz and zircon (Table 1), have higher Zr-concentrations (63–84 ppm), corresponding to temperatures of  $531\text{--}550 \pm 29^\circ\text{C}$  which is comparable to previous estimates for similar samples ( $470\text{--}520^\circ\text{C}$ ; Miller et al., 2009). Similar Zr-in-rutile temperature estimates of  $445\text{--}505^\circ\text{C}$  have also been obtained by Spear et al. (2006) for rutile from comparable ophiolites on the nearby island of Sifnos.

Unlike rutile from Syros, rutile from the Sesia Zone samples all grew in coexistence with quartz and zircon (Table 1). Samples MK52 and MK195 have Zr concentrations of 41–55 ppm, corresponding to a temperature range of  $503\text{--}525 \pm 28^\circ\text{C}$  (Table 3). Samples MK30, MK126, MK162 and MK541 have higher Zr-concentrations ranging between 73–120 ppm, resulting in higher temperatures which average around  $542\text{--}560 \pm 29^\circ\text{C}$  (Table 3). All samples yield temperatures that are within uncertainty of the broad range of estimates from the literature ( $550\text{--}620^\circ\text{C}$ ; Rubatto et al., 1999).

**Table 3**

Average Zr-in-rutile temperatures and results of conventional geobarometry on mineral inclusions using the jadeite-in-cpx (Holland, 1983) and Si-in-phengite (Massonne and Schreyer, 1989) geobarometers. For individual Zr-in-rutile temperature estimates see supplementary data (Table B.1).

Locality	Thermometry (°C)		Barometry (kbar)					
	Watson et al. (2006)		Tomkins et al. (2007)		Jd-in-cpx		Si-in-phengite	
	Average Temp	n	Inclusions	Matrix	Inclusions	Matrix		
<i>Syros, Greece</i>								
SY20 <sup>a,b</sup>				13				
SY440 <sup>a,b</sup>	509	20		13				
SY507 <sup>a,b</sup>	515	11		13				
SY545	657	3						
<i>Sesia Lanzo, Western Alps</i>								
MK30	551	13						
MK52	514	21						
MK126	538	9						
MK162	560	10		14				
MK195	513	12		13				
MK541	557	8						
<i>Dora-Maira, Western Alps</i>								
15623a	590	6						
19296a	620	12						
19464	586	15	667					
				27			30	

<sup>a</sup> No zircon.

<sup>b</sup> No quartz.

Rutiles separates from Parigi, taken from both the matrix (19464) and from within garnet megablasts (15623a), have similar Zr-concentrations ranging between 134–161 ppm which yield temperatures of 586–589 ±30 °C (Table 3). Higher Zr-concentrations of 214–240 ppm are recorded within rutile inclusions within garnet megablasts from Tapina (19296a), corresponding to slightly higher temperatures of 613–625 ±30 °C (Table 3). Despite rutile coexisting with quartz and zircon in two of the Dora-Maira samples (Table 1), these results are systematically lower than previous literature estimates (720–800 °C; Schertl et al., 1991; Nowlan et al., 2000). The presence of UHP mineral inclusions in the Dora-Maira samples however, also helps to constrain minimum P-T estimates. The identification of pyrope and coesite within rutile from sample 19464 indicates that these samples underwent ultra-high pressure conditions of at least 29 kbar (Fig. 6). Calculations made with the pressure-dependent coesite calibration of Tomkins et al. (2007) gives a temperature of 667 °C (Fig. 6; Table 3) and is similar to independent P-T estimates for these rocks.

## 6.2. Conventional geobarometry on mineral inclusions

As discussed previously, there is currently no independent method of determining pressures within rutile. The discovery of high-pressure phases as inclusions within rutile, however, suggests that in specific cases it may be possible to apply conventional geobarometry. To demonstrate this, the jadeite-in-omphacite and silica-in-phengite geobarometers have been applied to samples from the Sesia Zone and Dora-Maira. Calculations have been made using the temperatures obtained from Zr-in-rutile thermometry and by assuming that the target phases are in chemical equilibrium with the respective buffering phases.

The jadeite component of pyroxenes can be used as a geobarometer in blueschist- to eclogite-facies rocks to provide minimum pressures (Holland, 1983). This has been applied to omphacite inclusions found in samples MK162 and MK195 from the Sesia Zone, which are coexistent with quartz and albite (Table 1). Omphacite in these samples have a high jadeite content of Jd<sub>53</sub> Di<sub>47</sub> and Jd<sub>65</sub> Di<sub>35</sub> respectively, therefore the model for ordered omphacite with a composition close to Jd<sub>50</sub> Di<sub>50</sub> (Holland, 1983; their Fig. 10a) was used. Using temperatures obtained from Zr-in-

rutile thermometry (Table 3), sample MK162 yields a minimum pressure of 14 kbar at 560 °C, while MK195 gives a minimum pressure of 13 kbar at 513 °C (Fig. 6; Table 3). These estimates are in agreement with other minimum pressure estimates (>11 kbar) obtained for similar rocks from the Sesia Zone (Compagnoni et al., 1977; Pognante, 1989; Tropper et al., 1999). Omphacite is also found in the Syros samples, but estimates could not be calculated as they do not have the required buffering assemblage.

The Si-in-phengite geobarometer of Massonne and Schreyer (1989; their Fig. 5) is also widely used in metamorphic rocks and is calibrated for phengite coexisting with talc, kyanite and quartz/coesite within a P-T range of 15–40 kbar at 550–800 °C. Rutiles from sample 19464 (Dora-Maira) contain inclusions of all four minerals of the limiting assemblage (Table 1). Using an average temperature of 585 °C obtained by Zr-in-rutile thermometry, and an Si value of 3.43 a.p.f.u. from phengite inclusions (Table 2), the recalculated isopleths of Coggon and Holland (2002; their Fig. 4a) gives a pressure of ~27 kbar (Table 3). In comparison, the maximum Si value of phengite within the matrix of this sample of 3.49 a.p.f.u. gives a pressure of 30 kbar.

## 6.3. Average P-T calculations on inclusions within rutile (Sesia Zone)

In order to determine if additional P-T information can be obtained using mineral inclusions in samples where evidence of HP events have been partially obliterated in the matrix, average pressure (AvP) and average pressure-temperature (AvPT) calculations were performed on mineral inclusion assemblages using the software THERMOCALC v3.33 and the internally consistent thermodynamic database (Holland and Powell, 1998, recent upgrade). This method was successfully applied to three samples from the Sesia Zone. Mineral inclusion assemblages found in other samples did not permit these calculations due to an insufficient number of end-members. Calculations were made using mineral inclusions present within rutile (plus rutile and H<sub>2</sub>O), assuming that the inclusions were equilibrated under the same conditions. One exception has been made as titanite is not a common phase in equilibrium with rutile in this type of assemblage and therefore has been assumed to be an early phase. For more details regarding the method used

**Table 4**

Results of AvPT and AvP calculations obtained using THERMOCALC v3.33 software (Holland and Powell, 1998). For individual reactions see Table 4. Abbreviations: standard deviation (sd), correlation coefficient (Cor) and the significant fit statistical parameter (Sigfit).

Sample		XH <sub>2</sub> O	T (°C)	sd	P (kbar)	sd	Cor	Sigfit	Reactions
MK52	AvP	1.0	513 <sup>a</sup>		10.2	0.6	1.15	1–5	
	AvPT	1.0	549	16	10.9	0.9	0.43	1.27	2–3, 6–8
MK162	AvP	1.0	560 <sup>a</sup>		12.6	0.8	2.06	9–15	
	AvPT	1.0	613	36	14.0	1.2	0.76	1.84	9–15
MK195	AvPT	1.0	609	42	14.5	1	0.75	2.34	16–22

<sup>a</sup> Zr-in-rutile temperatures (Table 3).

and a list of independent reactions please see supplementary materials (Appendix C).

Average pressures are calculated over a known temperature range and as temperatures are usually better known than pressures (Powell and Holland, 1994), AvP calculations were calculated for two samples from the Sesia Zone using temperature obtained from Zr-in-rutile thermometry (Table 4). A pressure of  $12.6 \pm 0.8$  kbar was obtained for sample MK162 which is within uncertainty of published estimates (11–23 kbar; e.g. Konrad-Schmolke et al., 2006). A pressure estimate of  $10.2 \pm 0.6$  kbar was obtained for sample MK52 which is slightly lower than these estimates.

AvPT calculations were performed on samples from the Sesia Zone (Table 4). P-T estimates for MK162 and MK195 give results of  $613 \pm 36$  °C and  $14 \pm 1.2$  kbar, and  $609 \pm 42$  °C and  $14.5 \pm 1$  kbar respectively which are within uncertainty of previous estimates of peak conditions of 500–600 °C at 11–23 kbar (e.g. Konrad-Schmolke et al., 2006). The P-T estimate for sample MK52 of  $549 \pm 16$  °C and  $10.9 \pm 0.9$  kbar is also in good agreement, even if the pressure obtained is at the lower end of previous estimates.

## 7. Discussion

### 7.1. Preservation of high-pressure phases in rutile

Why is it such a surprise that rutile is a good container for mineral inclusions? Although rutile is known to be idiomorphic and resistant to fluid infiltration and re-equilibration at lower pressure conditions (Zack et al., 2004; Triebold et al., 2007), properties similar to those of garnet and zircon, it has a good cleavage and a tendency for twinning. These inherent anisotropies suggest that rutile could have a mechanical weakness and potential planes operating as preferential pathways for diffusion, which might inhibit the preservation of mineral inclusions. However, the lack of any observed reactions (as topotactic replacement), or distinct parting in BSE at high magnifications along the cleavage, is good evidence that although rutile is cleaved, it does not appear to be a major weakness or a pathway for preferential retrogression. Another factor to consider, particularly in preservation of UHP phases, is compressibility. Garnet and zircon both have a low compressibility which makes them a good container of phases such as coesite and microdiamond (e.g. Mosenfelder et al., 2005). Their remarkable confining strength means that they act as ‘pressure vessels’ and exert an overpressure on inclusions even when the rocks have been exhumed to the Earth’s surface. The occurrence of monomineralic coesite inclusions in rutile from the Dora-Maira massif suggests that this is also the case for rutile, and that it could be just as good of a container for other UHP minerals.

Our observations show that rutile is a good container for inclusions and that inclusions generally match the assemblage of the matrix minerals (Fig. 2; Tables 1 and 2), preserving a range of HP-UHP phases from the respective rocks. However, rutile growth can also occur along the prograde path, therefore the inclusion assemblage is not always a proxy for the peak metamorphic assemblage.

Indeed, in addition to peak HP-UHP phases, there is also evidence of prograde phases being preserved such as titanite within rutile in sample SY545 from Syros and corundum within sample 19464 from the Dora-Maira massif (Table 1). In each case the inclusions are monomineralic, completely surrounded by rutile and are crack-free. With regards to the corundum inclusions in sample 19464 (Dora-Maira), corundum is not present within the matrix and the texture and morphology of the inclusions are not consistent with exsolution lamellae (Fig. 2). Inclusions of corundum within magnesiostaurolite have previously been reported by Simon et al. (1997), taken from within a near end-member pyrope garnet from the Dora-Maira massif. They suggested that there may have been an earlier aluminium-rich and originally corundum-bearing subsystem, in which the magnesiostaurolite overgrew the corundum (Simon et al., 1997). Although the potential preservation of prograde minerals is an enticing way of constraining the prograde P-T path, their presence also demonstrates that careful consideration of the quasi-equilibrium mineral inclusion and host rutile assemblage is required.

The careful study of mineral inclusions within rutile can also help determine the metamorphic facies of the host rock (Fig. 6). Inclusions of glaucophane are indicative of blueschist-facies conditions, whereas, inclusions of garnet and omphacite (without albite) indicate eclogite-facies metamorphism. Transitional blueschist–eclogite facies rocks, such as those from the Sesia Zone, may contain inclusions of both glaucophane and omphacite depending on H<sub>2</sub>O activity.

### 7.2. Rutile: a repository for evidence of ultra-high pressure metamorphism?

UHP metamorphic mineral assemblages are often replaced during retrograde metamorphism due to hydration and re-equilibration during exhumation (Katayama and Maruyama, 2009). As a result, mineralogical evidence of UHP metamorphism has largely been restricted to armoured inclusions found in refractory minerals such as garnet and zircon (Parkinson and Katayama, 1999; Katayama and Maruyama, 2009). In this contribution it is shown that rutile from the UHP rocks of the Dora-Maira massif is also capable of retaining UHP inclusions such as coesite, pyrope and high-Si-phengite.

Coesite in Dora-Maira was first identified within pyrope garnet as bimimetic inclusions rimmed with palisade quartz (Chopin, 1984; Boyer et al., 1985) and later as micro-inclusions within zircon (Schertl and Schreyer, 1996). In the present study a number of coesite inclusions within rutile (Fig. 3), confirmed using Raman spectroscopy, show no visible fractures or transformation to quartz. The fact that these inclusions are untransformed and monomineralic implies that there was very little or no aqueous fluid present within the enclosing rutile (Parkinson and Katayama, 1999; Katayama and Maruyama, 2009), or that rutile had simply protected its interior from external fluids. The main Raman peak

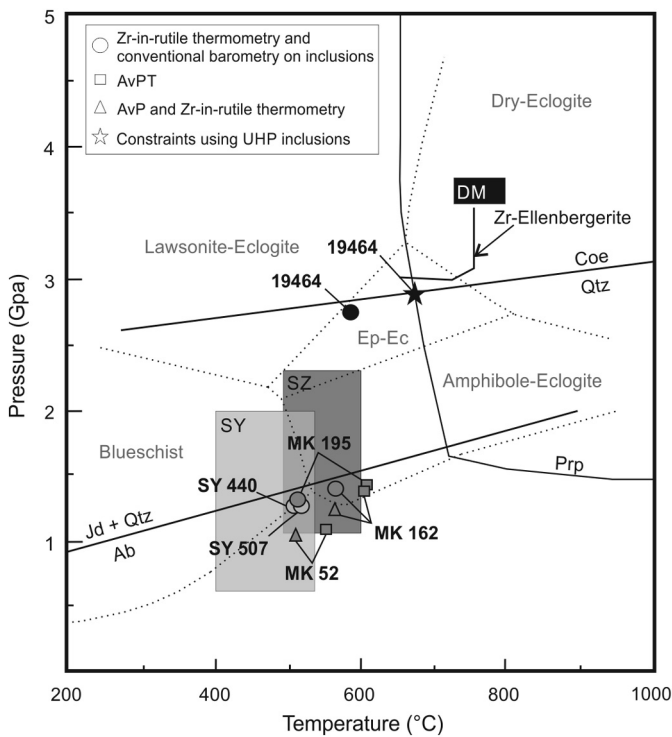


**Fig. 6.** Diagram showing  $P$ - $T$  estimates obtained from rutile and its mineral inclusions using a combination of geothermobarometric methods (errors included within the size of the symbols). Literature estimates are depicted by the large transparent boxes for Syros (SY), the Sesia Zone (SZ) and the Dora-Maira massif (DM).

for bimineralic coesite inclusions in garnet occurs at  $521\text{ cm}^{-1}$  (Boyer et al., 1985), however in this study the main peak obtained for monomineralic coesite inclusions occurs at  $523\text{ cm}^{-1}$  (Fig. 3) which is comparable to peaks obtained for similar inclusions in zircon from the Kokchetav massif (Parkinson and Katayama, 1999). The displacement of the Raman peaks to slightly higher frequencies can be explained by the pressure dependency in untransformed coesite. The host, in this case rutile, has a low compressibility and acts as a robust pressure vessel, therefore the inclusions are still subjected to  $P$ - $T$  conditions on or close to the coesite-quartz boundary (Parkinson and Katayama, 1999). These findings confirm that rutile can protect UHP minerals from late-stage overprinting and demonstrates its great potential as a repository for evidence of UHP metamorphism, especially in otherwise retrogressed samples.

### 7.3. Determining $P$ - $T$ conditions

Analysis of mineral inclusions shows that they have comparable chemical compositions to matrix minerals (Figs. 4 and 5; Table 2); therefore, it may be possible to obtain additional  $P$ - $T$  information from inclusions to further constrain the conditions of rutile growth and thus the metamorphic conditions within the host rock.

The first step is to apply the reliable Zr-in-rutile geothermometer. In this study, rutile equilibrated with zircon  $\pm$  quartz is demonstrated by the mineral constituents of the matrix of the respective samples. Quartz and zircon were also identified as inclusions within rutile (Table 1), which is a novel approach to confirm their presence as it is not always possible to assess if the rutile grew in coexistence with zircon and quartz, particularly in detrital populations. Overall, the temperature estimates obtained for rutile from Syros and the Sesia Zone (Table 3) are all within uncertainty of previous estimates (Fig. 6; Table 1), but those for rutile from the Dora-Maira massif are significantly lower than expected, due to the lack of a pressure term in this calibration (Watson et al., 2006).

However, as demonstrated in section 6.1, the occurrence of ultra-high pressure inclusions within rutile can optimise  $P$ - $T$  calculations for ultra-high pressure rocks by using the coesite calibration of Tomkins et al. (2007). This method should therefore be routinely used and  $\text{SiO}_2$  inclusions sought after (and their polymorph determined) when studying strongly retrogressed metamorphic rocks or detrital rutiles. It is also advised to use matrix phases alongside mineral inclusions if the host rock is known. For example, the occurrence of ellenbergerite inclusions alongside rutile within the pyrope megablasts helps to place a maximum temperature on the conditions of rutile growth within the Dora-Maira massif. Ellenbergerite, like rutile, grew during prograde metamorphism, directly followed by the formation of the pyrope megablasts, with the smaller pyrope crystals forming much later. The temperature stability of Zr-ellenbergerite ranges from approximately  $650\text{--}750\text{ }^\circ\text{C}$  (Brunet et al., 1998), therefore our temperature estimate of  $667\text{ }^\circ\text{C}$  obtained using the Zr-in-rutile calibration of Tomkins et al. (2007) is reasonable (Table 3).

Having determined temperatures using rutile geochemistry, the occurrence of certain HP-UHP mineral inclusions within rutile and their comparable chemical composition to matrix phases (Table 2) justifies the application of conventional geobarometry. Appropriate geobarometers for this study were found to be the jadeite-in-clinopyroxene geobarometer, which was applied to two samples from the Sesia Zone, and the Si-in-phengite geobarometer, which was applied to one sample from the Dora-Maira massif (Table 3). Fig. 6 summarises how pressure estimates obtained from mineral inclusions, when used in conjunction with Zr-in-rutile thermometry, produce  $P$ - $T$  estimates comparable to previous literature estimates for HP rocks from Syros and the Sesia Zone. In addition, it shows that the AvPT estimates obtained for suites of mineral inclusions within rutile from the Sesia Zone, produce  $P$ - $T$  estimates that are within uncertainty of previous estimates. This approach can currently only be applied when there are sufficient end-members allowing calculations (using inclusions from more than 1 grain) and where the host rock is known. This could therefore be of particular use for retrogressed samples, where conventional geothermobarometry using equilibrium rock-forming minerals is difficult or impossible. However, it is important to note that this method is not transferable to detrital populations as a full assemblage containing a suitable range of inclusions is unlikely to be present within a single grain.

### 7.4. Searching for inclusions in detrital populations

Rutile is one of the most physically and chemically stable heavy minerals in the sedimentary environment and has already been established as a key mineral in sediment provenance analysis as it is able to retain geochemical information from the source rock (e.g. Zack et al., 2004; Triendl et al., 2007). This study shows that mineral inclusions can preserve evidence of (U)HP metamorphism and can be used to determine the metamorphic conditions of the host rock. Therefore, there is the potential to use mineral inclusions in conjunction with U-Pb geochronometry, Zr-in-rutile geothermometry and the Nb/Cr discrimination diagram to identify source rocks and to find evidence of (U)HP events in potentially eroded or unexposed source areas.

To assess the feasibility of searching for inclusions in detrital rutile, we have started to analyse detrital rutile from modern river sediments collected in the Po River within the Po Plain at Casale Monferrato. This part of the river captures detritus from a wide area of the western Alps, including the Sesia Zone and the Dora-Maira massif. The detrital grains studied are well-rounded with abraded surfaces, thus representing material transported by riverine processes. In the supplementary materials (Fig. D.1; Table D.2), it is shown that detrital rutiles from the Po River contain a va-

riety of mineral inclusions and that the inclusions present (e.g. glaucophane, omphacite and garnet) are comparable to the types of inclusions found in the samples used in this study. As with grains from the whole rocks analysed in this study, detrital rutiles from the Po River have not been fractured along cleavage or twin planes, despite being transported at least 50–100 km from any likely source area. These early results are encouraging, although additional analysis is required to compare the composition of key primary phases to samples from the Sesia Zone and the Dora-Maira massif to determine if either of these terranes are the source of the rutile.

## 8. Conclusions

This study demonstrates that rutile can preserve mineral inclusions which faithfully record evidence of HP-UHP metamorphic events. Our main conclusions, along with aspects requiring caution and further study, are summarised below.

- Mineral inclusion assemblages generally match the matrix mineralogy and that  $P-T$  information obtained from inclusions relates to the conditions of rutile growth.
- Rare prograde minerals are preserved (corundum, titanite), indicating that rutile is capable of preserving mineral inclusions from different metamorphic stages of the  $P-T$  evolution.
- Mineral inclusions help to further constrain Zr-in-rutile temperatures and in some cases confirm the presence of zircon and quartz in co-existence with rutile.
- Pressure estimates can also sometimes be obtained by applying conventional geobarometry to mineral inclusion assemblages found within rutile.
- The preservation of minerals diagnostic of UHP conditions such as high-Si phengite, pyrope and coesite suggests that rutile is an excellent repository to look for evidence of UHP metamorphism, the implications of which may profoundly change the way we investigate HP-UHP metamorphism in partially retrograde samples.
- Further work on detrital rutiles from a variety of sedimentary basins of different ages may help to better constrain the secular evolution of (U)HP metamorphism on Earth.

## Acknowledgements

We would firstly like to thank Thomas Zack and an anonymous reviewer for their constructive reviews that helped to improve the manuscript. We also thank Horst Marschall, Matthias Konrad-Schmölk and Florentina Enea for providing us with the samples used in this study, Stuart Kearns at the University of Bristol for his assistance using the electron microprobe and Mike Fowler for his suggestions and proof-reading. This project was funded by Natural Environment Research Council grant NE/I025573 awarded to PI Storey, including a NERC studentship for Emma Hart.

## Appendix A. Supplementary material

Supplementary material related to this article can be found online at <http://dx.doi.org/10.1016/j.epsl.2016.04.035>.

## References

- Boyer, H., Smith, D.C., Chopin, C., Lasnier, B., 1985. Raman microprobe (RMP) determinations of natural and synthetic coesite. *Phys. Chem. Miner.* 12, 45–48.
- Brunet, F., Chopin, C., Seifert, F., 1998. Phase relations in the  $MgO-P_2O_5-H_2O$  system and the stability of phosphoellenbergerite: petrological implications. *Contrib. Mineral. Petro.* 131, 54–70.
- Chopin, C., Henry, C., Michard, A., 1991. Geology and petrology of the coesite-bearing terrain, Dora-Maira massif, Western Alps. *Eur. J. Mineral.* 3, 263–291.
- Chopin, C., 1984. Coesite and pure pyrope in high-grade blueschists of the western Alps: a first record and some consequences. *Contrib. Mineral. Petro.* 86, 107–118.
- Coggon, R., Holland, T.J.B., 2002. Mixing properties of phengitic micas and revised garnet-phengite thermobarometers. *J. Metamorph. Geol.* 20, 683–696.
- Compagnoni, R., Messiga, B., Castelli, D., 1994. High pressure metamorphism in the Western Alps. In: Guide-Book to the Field Excursion of the 16th Meeting of the IMA. Pisa, September 10–15, 2004. 148 p.
- Compagnoni, R., Dal Piaz, G.V., Hunziker, J.C., Goso, G., Lombardo, B., Williams, P.F., 1977. The Sesia-Lanzo zone, a slice of continental crust with alpine high pressure-low temperature assemblages in the Western Italian Alps. *Rend. Soc. Ital. Mineral. Petro.* 33, 281–334.
- Dhuime, B., Hawkesworth, C.J., Cawood, P.A., Storey, C.D., 2012. A Change in the Geodynamics of Continental Growth 3 Billion Years Ago. *Science* 335, 1334–1336.
- Duchêne, S., Lardeaux, J.-M., Albarède, F., 1997. Exhumation of eclogites: insights from depth-time path analysis. *Tectonophysics* 280, 125–140.
- Gasco, I., Gattiglio, M., Borghi, A., 2013. Review of metamorphic and kinematic data from Internal Crystalline Massifs (Western Alps): PT paths and exhumation history. *J. Geodyn.* 63, 1–19.
- Gebauer, D., Schertl, H.-P., Brix, M., Schreyer, W., 1997. 35 Ma old ultrahigh-pressure metamorphism and evidence for very rapid exhumation in the Dora Maira Massif, Western Alps. *Lithos* 41, 5–24.
- Holland, T.J.B., Powell, R., 1998. An internally consistent thermodynamic data set for phases of petrological interest. *J. Metamorph. Geol.* 16, 309–343.
- Holland, T.J.B., 1983. The experimental determination of activities in disordered and short-range ordered jadeitic pyroxenes. *Contrib. Mineral. Petro.* 82, 214–220.
- Katayama, I., Maruyama, S., 2009. Inclusion study in zircon from ultrahigh-pressure metamorphic rocks in the Kokchetav Massif: an excellent tracer of metamorphic history. *J. Geol. Soc. Lond. Spec. Publ.* 166, 783–796.
- Konrad-Schmölk, M., Babist, J., Handy, M.R., O'Brien, P.J., 2006. The physico-chemical properties of a subducted slab from garnet zonation patterns (Sesia Zone, Western Alps). *J. Petrol.* 47, 2123–2148.
- Marschall, H.R., Ludwig, T., Altherr, R., Kalt, A., Tonarini, S., 2006. Syros metasomatic tourmaline: evidence for very high- $\delta^{11}B$  fluids in subduction zones. *J. Petrol.* 47, 1915–1942.
- Maruyama, S., Liou, J.G., Terabayashi, M., 1996. Blueschists and eclogites of the world and their exhumation. *Int. Geol. Rev.* 8, 485–594.
- Massonne, H.-J., Schreyer, W., 1989. Stability field of the high-pressure assemblage talc + phengite and two new phengite barometers. *Eur. J. Mineral.* 1, 391–410.
- Meinhold, G., 2010. Rutile and its application in earth sciences. *Earth-Sci. Rev.* 102, 1–28.
- Miller, D.P., Marschall, H.R., Schumacher, J.C., 2009. Metasomatic formation and petrology of blueschist-facies hybrid rocks from Syros (Greece): implications for reactions at the slab-mantle interface. *Lithos* 107, 53–67.
- Mosenfelder, J.L., Schertl, H.-P., Smyth, J.R., Liou, J.G., 2005. Factors in the preservation of coesite: the importance of fluid infiltration. *Am. Mineral.* 90, 779–789.
- Nowlan, E.U., Schertl, H.-P., Schreyer, W., 2000. Garnet-omphacite-phengite thermobarometry of eclogites from the coesite-bearing unit of the southern Dora Maira Massif, Western Alps. *Lithos* 52, 197–214.
- Okrusch, M., Bröcker, M., 1990. Eclogites associated with high-grade blueschists in the Cyclades archipelago, Greece: a review. *Eur. J. Mineral.* 2, 451–478.
- Palin, R.M., White, R.W., 2016. Emergence of blueschists on Earth linked to secular changes in oceanic crust composition. *Nat. Geosci.* 9, 60–64.
- Parkinson, C.D., Katayama, I., 1999. Present-day ultrahigh-pressure conditions of coesite inclusions in zircon and garnet: evidence from laser Raman microscopy. *Geology* 27, 979–982.
- Pognante, U., 1989. Lawsonite, blueschist and eclogites formation in the southern Seisa Zone (Western Alps, Italy). *Eur. J. Mineral.* 1, 89–104.
- Powell, R., Holland, T., 1994. Optimal geothermometry and geobarometry. *Am. Mineral.* 79, 120–133.
- Rubatto, D., Gebauer, D., Compagnoni, R., 1999. Dating of eclogite-facies zircons: the age of Alpine metamorphism in the Sesia-Lanzo Zone (Western Alps). *Earth Planet. Sci. Lett.* 167, 141–158.
- Schertl, H.-P., Schreyer, W., 2008. Geochemistry of coesite-bearing pyrope quartzites and related rocks from the Dora-Maira Massif, Western Alps. *Eur. J. Mineral.* 20, 791–809.
- Schertl, H.-P., Schreyer, W., 1996. Mineral inclusions in heavy minerals of the ultrahigh-pressure metamorphic rocks of the Dora-Maira Massif and their bearing on the relative timing of petrological events. Isotopic studies of crust–mantle evolution. In: Basu, A., Hart, S.R. (Eds.). *Earth Processes: Reading the Isotopic Code*. In: *Geophys. Monogr.*, vol. 95. AGU, pp. 331–342.
- Schertl, H.-P., Schreyer, W., Chopin, C., 1991. The pyrope-coesite rocks and their country rocks at Parigi, Dora-Maira Massif, Western Alps: detailed petrography, mineral chemistry and PT path. *Contrib. Mineral. Petro.* 108, 1–21.
- Schmid, S.M., Fügenshuh, B., Kissling, E., Schuster, R., 2004. Tectonic map and overall architecture of the Alpine orogen. *Eclogae Geol. Helv.* 97, 93–117.
- Simon, G., Chopin, C., Schenk, V., 1997. Near-end-member magnesiochloritoid in prograde-zoned pyrope, Dora-Maira massif, Western Alps. *Lithos* 41, 37–57.

- Smart, K.A., Tappe, S., Stern, R.A., Webb, S.J., Ashwal, L.D., 2016. A review of the isotopic and trace element evidence for mantle and crustal processes in the Hadean and Archean: implications for the onset of plate tectonic subduction. *Nat. Geosci.* 9, 255–259.
- Spear, F.S., Wark, D.A., Cheney, J.T., Schumacher, J.C., Watson, E.B., 2006. Zr-in-rutile thermometry in blueschists from Sifnos, Greece. *Contrib. Mineral. Petrol.* 152, 375–385.
- Stern, R.J., 2005. Evidence from ophiolites, blueschists and ultrahigh-pressure metamorphic terranes that the modern episode of subduction tectonics began in Neoproterozoic time. *Geology* 33, 557–560.
- Stern, R.J., Tsujimori, T., Harlow, G., Groat, L.A., 2013. Plate tectonic gemstones. *Geology* 41, 723–726.
- Tomaschek, F., Kennedy, A.K., Villa, I.M., Lagos, M., Ballhaus, C., 2003. Zircons from Syros, Cyclades, Greece – recrystallization and mobilization of zircon during high-pressure metamorphism. *J. Petrol.* 44 (11), 1977–2002.
- Tomkins, H.S., Powell, R., Ellis, D.J., 2007. The pressure dependence of the zirconium-in-rutile thermometer. *J. Metamorph. Geol.* 25, 703–713.
- Triebold, S., von Eynatten, H., Luvizotto, G.L., Zack, T., 2007. Deducing source rock lithology from detrital rutile geochemistry: an example from the Erzgebirge, Germany. *Chem. Geol.* 244, 421–436.
- Tropper, P., Essene, E.J., Sharp, Z.D., Hunziker, J.C., 1999. Application of K-feldspar-jadeite-quartz barometry to eclogites facies metagranites and metapelites in the Seisa Lanzo Zone (Western Alps, Italy). *J. Metamorph. Geol.* 17, 195–209.
- Trotet, F., Jolivet, L., Vidal, O., 2001. Tectono-metamorphic evolution of Syros and Sifnos islands (Cyclades, Greece). *Tectonophysics* 338, 179–206.
- Watson, E.B., Wark, D.A., Thomas, J.B., 2006. Crystallization thermometers for zircon and rutile. *Contrib. Mineral. Petrol.* 151, 413–433.
- Whitney, D.L., Evans, B.W., 2010. Abbreviations for names of rock-forming minerals. *Am. Mineral.* 95, 185–187.
- Zack, T., Eynatten, H.V., Kronz, A., 2004. Rutile geochemistry and its potential use in quantitative provenance studies. *Sediment. Geol.* 171, 37–58.
- Zack, T., Stockli, D.F., Luvizotto, G.L., Barth, M.G., Belousova, E., Wolfe, M.R., Hinton, R.W., 2011. In situ U-Pb rutile dating by LA-ICP-MS: Pb-208 correction and prospects for geological applications. *Contrib. Mineral. Petrol.* 162, 515–530.